Mechanism for the Gas-Phase Reaction between Formaldehyde and Hydroperoxyl Radical. A Theoretical Study

Josep M. Anglada* and Victor M. Domingo

Departament de Química Orgànica Biològica, Institut d'Investigacions Químiques i Ambientals de Barcelona, IIQAB−CSIC, c/Jordi Girona 18, E08034 Barcelona, Spain

Received: July 20, 2005; In Final Form: September 30, 2005

We present a high-level theoretical study on the gas-phase reaction between formaldehyde and hydroperoxyl radical carried out using the DFT-B3LYP, QCISD, and CCSD(T) theoretical approaches in connection with the 6-311+G(d,p), 6-311+G(2df,2p), and aug-cc-pVTZ basis sets. The most favorable reaction path begins with the formation of a pre-reactive complex and produces the peroxy radical $CH_2(OO)OH$ in a process that is computed to be exothermic by 16.8 kcal/mol. This reaction involves a process in which the oxygen terminal of the HO_2 moiety adds to the carbon of formaldehyde, and, simultaneously, the hydrogen of the hydroperoxyl group is transferred to the oxygen of the carbonyl in a proton-coupled electron-transfer mechanism. Our calculations show that this transition state lies below the sum of the energy of the reactants, and we computed a rate constant at 300 K of 9.29×10^{-14} cm^3 molecule^{-1} s^{-1}, which is in good agreement with the experimental results. Also of interest in combustion chemistry, we studied the hydrogen abstraction process by HO_2, the result of which is the formation of $HCO + H_2O_2$. We found two reaction paths with activation enthalpies close to 12 kcal/mol. For this process, we computed a rate constant of 1.48×10^{-16} cm^3 molecule^{-1} s^{-1} at 700 K, which also agrees quite well with experimental results.

Introduction

Formaldehyde is among the most reactive organic contaminants in the atmosphere, with concentration levels up to 150 ppb in air-polluted areas.[1] It is emitted to the troposphere directly from motor vehicles and from industrial emissions, and it is also formed by the oxidation of volatile organic compounds.[2−5] In the atmosphere, H_2CO reacts mainly with hydroxyl radical in a process that involves a direct hydrogen abstraction, whereas the OH addition channel has been found to be unfavorable.[6,7]

The reaction of formaldehyde with hydroperoxyl radical also plays a significant role, mainly in polluted atmospheres in which the ratio between HO_2 and HO radicals is high. For this reaction, rate constants for the 200−373 K temperature range have been reported, which have negative temperature dependence.[1,6,8−11] In contrast to the reaction with hydroxyl radical, the reaction between formaldehyde and hydroperoxyl radical is assumed to be an addition, and the following mechanism was first proposed:[12]

$$H_2CO + HO_2 \rightarrow CH_2(O)OOH \rightarrow CH_2(OO)OH \qquad (1)$$

Here, the alkoxy radical formed in the first step isomerizes to yield the peroxy radical. After performing thermochemical bond additive calculations and an apparent negative activation energy derived from the measured Arrhenius parameter, Veyret et al.[9] suggested that the alkoxy radical could be in equilibrium with the reactants, and the isomerization of this intermediate to the peroxy radical would occur via an energy barrier that would be slightly below the energy of the reactants. More recently Benson,[13] on the basis of thermochemical bond additive calculations, the derived equilibrium constants, and a point charge model for the interacting species, suggested that the addition of hydroperoxyl radical to formaldehyde could yield the peroxy radical $OOCH_2OH$ in a single step as described by eq 2.

$$H_2CO + HO_2 \rightarrow CH_2(OO)OH \qquad (2)$$

In fact, a reaction path for the direct formation of the peroxide radical according to eq 2 was already suggested theoretically by Evleth et al.,[14] who also proposed that the probable intermediate is a hydrogen-bonded complex between H_2CO and HO_2. This reaction path was reported indirectly in a theoretical study on the oxidation of the hydroxymethyl radical by molecular oxygen,[15,42] which also included a reaction path for the two-step mechanism pointed out in eq 1. Additional information about a pre-reactive hydrogen bond complex was reported recently in a theoretical study by Aloisio et al.[16]

A further interest in the reaction between formaldehyde and hydroperoxyl radical arises from its importance in combustion processes, where kinetic studies for the hydrogen abstraction process (eq 3) have been reported in the 641−2500 K temperature range.[6,17−19]

$$H_2CO + HO_2 \rightarrow HCO + H_2O_2 \qquad (3)$$

The scope of this work is to perform a detailed theoretical study on the reaction described by eqs 1−3 with the aim of clarifying the reaction mechanism.

Theoretical Methods

We employed different theoretical approaches in this study. In a first step, all geometry optimizations were carried out with the hybrid density functional B3LYP approach[20] in connection with the 6-311+G(2df, 2p) basis set.[21,22] At this level of treatment, we computed the harmonic vibrational frequencies

* Corresponding author. E-mail: anglada@iiqab.csic.es.

10.1021/jp054018d CCC: $30.25 © 2005 American Chemical Society
Published on Web 11/03/2005

to verify the nature of the corresponding stationary point and to provide the zero-point vibrational energy (ZPE) and the thermodynamic contributions to the enthalpy and free energy. Moreover, at this level of theory, we performed intrinsic reaction coordinate (IRC) calculations[23−25] to ensure that a given transition state connects the desired reactant and product.

In a second step, we also reoptimized all stationary points by using the QCISD[26] level of theory and the 6-311+G(d,p) basis set.[21,22] However, this basis set was found to be insufficient to obtain a correct description of several of the pre-reactive complexes found in this work (see below), and therefore we also re-optimized these complexes at the QCISD level of theory with the more flexible 6-311+G(2df,2p) basis set.

In a third step, and aiming to provide more reliable relative energies, we computed, at the optimized QCISD geometries, single-point CCSD(T)[27,28] energy calculations using the more flexible aug-cc-pVTZ basis set.[29,30] In these calculations, we took into account the value of the T1 diagnostic[31,32] in the CCSD wave function to assess the reliability of these calculations with regard to a possible multireference character of the wave function at the corresponding stationary point. In addition, the basis set superposition error (BSSE) according to the counterpoise method by Boys and Bernardi[33] was also calculated at this level of theory for all the complexes. All of these calculations were performed with the Gaussian 02 suit of programs.[34] The Molden program was also used to visualize the geometric and electronic features of the different stationary points.[35]

The bonding features of several stationary points of interest were analyzed by employing the atoms in molecules (AIM) theory by Bader.[36] This analysis was carried out over the first-order density matrix, obtained at the QCISD level of theory, by using the AIMPAC program package.[37]

In a final step, and for the reactions of interest, we carried out a kinetic study employing conventional transition-state theory. As these reactions begin with a formation of a barrierless pre-reactive complex prior to the transition state and the release of the products, every process can be described as a complex reaction, as described by eq 4, in which we assume that the complex is in equilibrium with the reactants.

$$H_2CO + HOO \underset{k_{-1}}{\overset{k_1}{\rightleftharpoons}} \text{pre reactive Complex} \xrightarrow{k_2} \text{Products} \qquad (4)$$

With this assumption, and according to the steady-state conditions, the rate constant for each process is given by eq 5.

$$k_I = \frac{k_1}{k_{-1}} k_2 = K_{eq} k_2 \qquad (5)$$

The equilibrium constant K_{eq} in the first step and the rate constant k_2 of the second step of eq 4 are given by eqs 6 and 7, respectively:

$$K_{eq} = \sigma \frac{Q_{Complex}}{Q_{H_2CO} Q_{HO_2}} \exp\frac{-(E_C - E_R)}{RT} \qquad (6)$$

$$k_2 = \kappa\sigma \frac{k_B T}{h} \frac{Q_{TS}}{Q_{Complex}} \exp\frac{-(E_{TS} - E_C)}{RT} \qquad (7)$$

in which the various Q values denote the partition functions of the reactants H_2CO and HOO, the pre-reactive complex, and the transition state; E_R, E_C and E_{TS} are the total energies of the reactants, the hydrogen bond complex, and transition state, respectively; k_B and h are the Boltzmann and Planck constants, respectively; σ is the symmetry number; and κ is the tunneling correction, which was computed by the zero-order approximation to the vibrationally adiabatic potential energy surface (PES) with zero curvature. An unsymmetrical Eckart potential energy barrier was used to approximate the potential energy curve.[43] The TheRate program was employed to carry out this kinetic study.[38]

Results and Discussion

Almost all of the elementary reactions considered in the present work begin with the formation of a pre-reactive complex that is designated by the prefix **Cr** followed by a number to differentiate one from each other. The transition states are designated by the prefix **TS** and a number, and some of the intermediates found in this work are designated by the letter **M** followed by a number. In the exit channels, there are also complexes occurring before the release of the products, which are labeled with the prefix **Cp** and a number. Figures 1, 4, and 5 show the most relevant geometrical parameters of the stationary points found in this work; Figures 2 and 3 schematically display the energetic profiles, along with the atom numbering of each stationary point; Table 1 gives the relative energies, enthalpies, and free energies; Table 2 shows the computed vibrational frequencies and IR intensities of the reactants and the pre-reactive complexes; and Tables 3 and 4 list the results of the kinetic study.

Throughout the text, only relative energetic values are reported. The corresponding absolute energies are provided as Supporting Information, along with the Cartesian coordinates of all stationary points reported in this work and the topological values of the AIM analysis of the wave function that was carried out.

Reactants and Pre-reactive Complexes. We found four complexes formed between the reactants H_2CO and HO_2. Three of them correspond to minima in the PES and have been designated as **Cr1**, **Cr2**, and **Cr3**, whereas the fourth is a transition state and has been labeled **TS9**. The most relevant geometrical parameters of the corresponding optimized structures are displayed in Figure 1 along with the optimized parameters of the H_2CO and HO_2 reactants, while Figure 2 shows a schematic energy profile corresponding to the region of the pre-reactive complexes.

Our calculations show that the most stable complex is **Cr1**, which has been reported recently in the literature.[14−16,42] In this complex, all of the atoms lie in the same plane, forming a six-membered-ring structure and therefore having C_S molecular symmetry (see Figure 1). The electronic state is $^2A''$ with the electronic configuration $14a'^2 2a''^2 3a''^1$, so that the unpaired electron of the HOO moiety resides in an orbital perpendicular to the molecular plane. This electronic characterization allows for the interaction of the H7 of formaldehyde with a lone pair of the terminal oxygen atoms of HOO, together with an interaction of the hydrogen of the hydroperoxyl radical moiety with a lone pair of the oxygen atoms of the carbonyl group, so that **Cr1** has two hydrogen bonds. These facts are confirmed by an AIM topological analysis of the wave function. This analysis reveals the presence of bond critical points (bcp), located between O1 and H7 [$\rho(r_{bcp}) = 0.0073$ e bohr^{-3} and $\nabla^2\rho(r_{bcp}) = 0.0258$ e bohr^{-5}] and between H3 and O4 [$\rho(r_{bcp}) = 0.0327$ e bohr^{-3} and $\nabla^2\rho(r_{bcp}) = 0.1072$ e bohr^{-5}], and these values for the density of the wave function and the Laplacian are characteristic of hydrogen bond interactions. In addition, a ring critical point was been found. Figure 1 shows that, at the

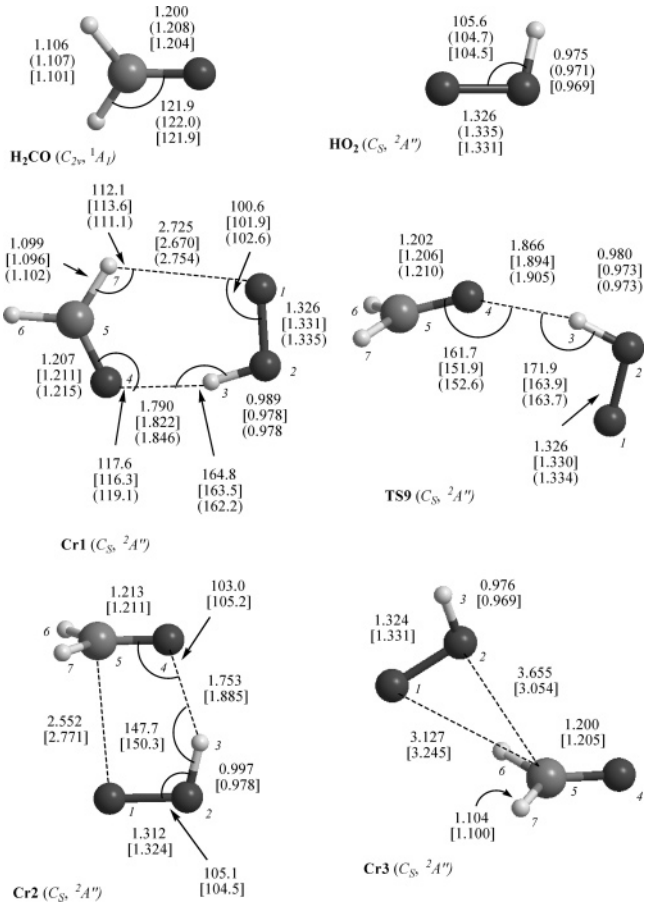

Figure 1. Selected geometrical parameters for the reactants and pre-reactive complexes, optimized at the B3LYP/6-311+G(2df,2p), QCISD/6-311+G(2df,2p) (in brackets), and QCISD/6-311+G(d,p) (in parentheses) levels of theory.

highest level of theory used in this work (QCISD/6-311+G-(2df,2p)), the two hydrogen bond lengths (O1···H7 and H3···O4) are computed to be 2.670 and 1.822 Å, respectively, and agree with the bond distances obtained at other levels of theory (see Figure 1) and with those reported in the literature.[14−16,42] These two hydrogen bond distances are very different, which suggests distinct strength for both interactions, as also pointed out by the values for the density of the wave function at the corresponding bcp. At the CCSD(T)/aug-cc-pVTZ level of theory, our calculations predict **Cr1** to have a dissociation energy of 7.4 kcal/mol, or 6.6 kcal/mol when the BSSE correction is accounted for (see Table 1 and Figure 2), values that agree quite well with those reported previously in the literature.[14−16, 42]

The pre-reactive **Cr2** complex also has C_S symmetry, and the electronic description corresponds to a $^2A''$ state ($13a'^2 3a''^2 4a''^1$). As shown in Figure 1, the plane of symmetry bisects the formaldehyde moiety, whereas the HOO moiety is contained in the molecular plane. In addition, the hydrogen of the HOO group points toward the oxygen of the carbonyl group so that the complex has a five-membered-ring structure. Moreover, the analysis of the wave function shows that the spin density of the unpaired electron is located over the HOO moiety in an orbital perpendicular to the symmetry plane, which leads to the interesting question of what kinds of interactions maintain the bonding of this complex. From a geometrical point of view, the results displayed in Figure 1 show that the optimized parameters are quite sensitive to the theoretical approach used, namely, the method and basis set, especially the H3O4 and O1C5 distances conforming the five-membered ring. The best level of theory employed in the optimization procedure, QCISD/6-311+G(2df,2p), predicts the distances to be 1.885 and 2.771 Å, respectively. In addition, the topological analysis of the wave function reveals the existence of two bcp, one located between H3 and O4 ($\rho(r_{bcp}) = 0.0256$ e bohr^{-3} and $\nabla^2\rho(r_{bcp}) = 0.0989$ e bohr^{-5}) and the other located between O1 and C5 ($\rho(r_{bcp}) = 0.0134$ e bohr^{-3} and $\nabla^2\rho(r_{bcp}) = 0.0463$ e bohr^{-5}), which allow us to classify the H3···O4 interaction as a hydrogen bond and the O1···C5 interaction as being of the van der Waals type. From a technical point of view, it is also interesting to compare these results with those obtained at others levels of theory. As shown in Figure 1, The B3LYP/6-311+G(2df,2p) level predicts slightly shorter H3O4 and O1C5 bond distances (1.753 and 2.552 Å, respectively), whereas, at the QCISD/6-311+(d,p) level of theory, the optimized structure results in atomic distances of 1.905 and 4.019 Å, respectively, the later being larger than the sum of the van der Waals radii of C and O. In fact, the geometry obtained at the QCISD/6-311+G(d,p) level of theory does not correspond to **Cr2**, but it corresponds to **TS9**, which is described below (see also Figures 1 and 2). Consequently, these results show the inability of the 6-311+G(d,p) basis set to describe the O1C5 van der Waals interaction and point out the importance of using sufficiently flexible basis sets to correctly describe complexes bound by small interactions. With regard to the stability of this complex, our calculations at the best level of treatment predict a dissociation energy for this complex of 5.5 kcal/mol (4.7 kcal/mol when the BSSE corrections are considered; see Table 1 and Figure 2). This complex may correspond to those reported recently by Dibble[42] and placed 1.2 kcal/mol above the lowest planar complex, although there are no geometrical parameters to compare them to. For this complex, Dibble[42] report a minima at the B3LYP/6-311++G(3df,3pd) level of theory but found a stationary point with a very small imaginary frequency at MP2/6-311++G(2d,2p). This result led us to optimize and characterize **Cr2** at the MP2/6-311+G(2df,-2p) level of theory, and we found it to be a minimum at the PES. This fact again points out the importance of the basis function (the polarization *f* functions in this case) in describing the weak interaction of these kinds of complexes.[45]

We found a further stationary point having the same symmetry (C_S), electronic description ($^2A''$ state, $13a'^2 3a''^2 4a''^1$), and orientation as that of **Cr2**; that is, the plane of symmetry bisects the formaldehyde moiety, whereas the HOO moiety is contained in the molecular plane. However, this stationary point has an imaginary frequency (118.2 cm^{-1}) and therefore corresponds to the transition state that has been labeled **TS9**. Figure 1 shows that there is a sole hydrogen bond interaction that occurs between the oxygen of the carbonyl group and the hydrogen of the hydroperoxyl radical (d(O4H3) = 1.866 Å), while the angle involving the hydrogen bond (O4H3O2) is close to 172°. Both the analysis of the transition vector and Figure 2 show that this transition state connects the two identical conformers of **Cr1**, and for this process, we computed, at the best level of treatment, an activation energy of 2.1 kcal/mol (see Table 1 and Figure 2). In addition to this transition state, we also looked for a possible transition state connecting **Cr1** and **Cr2**, but we were unsuccessful in finding it.

The third pre-reactive complex we found in this work is designated as **Cr3** in Figures 1 and 2. This complex has C_S symmetry and the electronic state is $^2A''$ with a $13a'^2 3a''^2 4a''^1$ electronic configuration. As for the **Cr2** complex, the HOO moiety is also contained in the symmetry plane, which bisects the formaldehyde moiety. However the hydrogen of the HOO

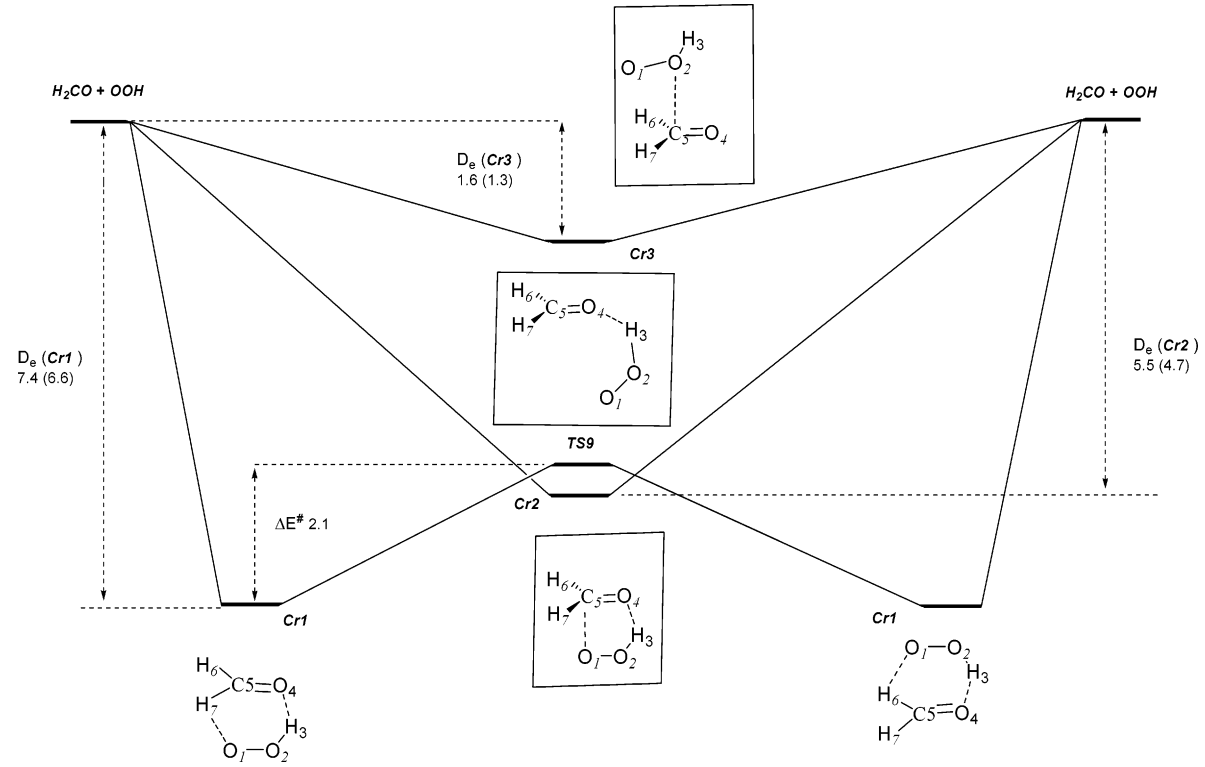

Figure 2. Energy profile for the pre-reactive complexes. Relative energies are in kcal/mol. D_e is the dissociation energy of the corresponding complex, and $\Delta E^{\#}$ is the activation barrier.

TABLE 1: Zero-Point Energies (ZPE), Entropies (*S*), Reaction and Activation Energies (*E*), ZPE-Corrected Energies (*E* + ZPE), Enthalpies (*H*), and Free Energies (*G*) for the Reaction between H_2CO and HO_2[a]

compounds	ZPE[b] (kcal/mol)	S^b (e.u.)	ΔE^c (kcal/mol)	ΔE + ZPE[c] (kcal/mol)	ΔH^c (kcal/mol)	ΔG^d (kcal/mol)
$H_2CO + HO_2$	25.5	108.3	0.0	0.0	0.0	0.0
Cr1	27.6	79.3	−9.4 (−8.6)	−7.4 (−6.6)	−7.7 (−6.9)	1.0 (1.8)
TS9	26.8	82.8	−6.7	−5.3	−5.6	1.9
Cr2	27.7	76.1	−7.6 (−6.8)	−5.5 (−4.7)	−6.0 (−5.2)	3.6 (4.4)
Cr3	26.2	96.1	−2.3 (−2.0)	−1.6 (−1.3)	−1.0 (−0.7)	2.6 (2.9)
TS1	26.6	67.4	−3.2	−2.1	−3.7	8.5
M3	30.4	69.6	−20.3	−15.4	−16.8	−5.2
TS8	26.4	68.3	23.1	24.0	22.5	34.4
Cp1	28.3	74.0	−67.4	−64.6	−65.4	−55.2
HCOOH + HO	26.4	101.9	−58.8	−57.9	−58.1	−56.2
TS4	27.9	70.2	16.9	19.3	18.1	29.4
TS6	27.0	71.7	21.4	22.9	21.8	32.7
M2b	28.6	69.8	−0.9	2.2	0.9	12.4
TS5	27.0	70.8	24.2	25.7	24.5	35.6
M2a	28.0	71.0	2.1	4.6	3.5	14.7
TS7	27.5	65.2	24.7	26.7	24.7	37.5
TS2	23.7	76.5	14.2	12.4	11.8	21.2
TS3	23.7	76.8	14.7	12.8	12.2	21.6
Cp2	26.1	85.8	−1.8 (−1.3)	−1.2 (−0.7)	−0.9 (−0.5)	5.8 (6.3)
$HCO + H_2O_2$	24.8	107.9	1.88	1.2	1.4	1.5

[a] Values in parenthesis include BSSE corrections. [b] Values obtained at B3LYP/6-311+G(2df,2p). [c] Energies at the CCSD(T)/aug-cc-pVTZ//QCISD/6-311+G(d,p) level. [d] Added to the *E* values and the ZPE, enthalpic, and entropic corrections obtained at B3LYP/6-311+G(2df,2p).

group is directed outward from the oxygen of the carbonyl group, so that no hydrogen-bond-type interaction is possible, and the complex is bonded by a van der Waals interaction. The optimized geometrical parameters displayed in Figure 1 show that, at the QCISD/6-311+G(2df,2p) level of theory, this van der Waals interaction occurs between O2 and C5 with a bond length of 3.054 Å (the corresponding topological parameters are $\rho(r_{bcp}) = 0.0050$ e bohr^{-3} and $\nabla^2\rho(r_{bcp}) = 0.0256$ e bohr^{-5}), whereas at the B3LYP/6-311+G(2df,2p) level of theory, the van der Waals interaction occurs between O1 and C5 with a bond length of 3.127 Å (the topological parameters are $\rho(r_{bcp}) = 0.0062$ e bohr^{-3} and $\nabla^2\rho(r_{bcp}) = 0.0249$ e bohr^{-5}). Despite this discrepancy, the CCSD(T)/aug-cc-pVTZ energy at both geometries is practically the same, pointing out the flat character of the PES. Table 1 and Figure 2 show that the computed binding energy of this complex is 1.6 kcal/mol (1.3 kcal/mol when the BSSE corrections are taken into account).

At this point, it is interesting to compare the relative stability of the three pre-reactive complexes described in this work. Although we computed relatively high binding energies for the hydrogen bond complexes **Cr1** and **Cr2** and a small binding energy for the van der Waals **Cr3** complex, the results displayed in Table 1 show the important differential entropic effects for these complexes, causing the equilibrium to be shifted to the

TABLE 2: Scaled Harmonic Frequencies (in cm^{-1})[a] and IR Intensities (in km mol^{-1}) Calculated at the B3LYP/6-311+G(2df,2p) Level of Theory

	H_2CO/HOO		Cr1		Cr2		Cr3	
approx. assgnmt	freq.	IR int.	freq.[b]	IR int.[c]	freq.[b]	IR int.[c]	freq[b]	IR int.[c]
hydroperoxyl OH stretch.	3469	28.2	3232 (−237)	676.0 (24.0)	3111 (−358)	116.9 (4.1)	3468 (−1)	37.1 (1.3)
CH2 asym. stretch.	2833	117.6	2913 (80)	34.0 (0.3)	2898 (65)	67.3 (0.6)	2846 (13)	109.0 (0.9)
CH2 sym. stretch.	2779	71.1	2826 (47)	73.5 (1.0)	2828 (49)	44.2 (0.6)	2789 (10)	73.5 (1.0)
CO stretch.	1746	116.1	1718 (−28)	108.1 (0.9)	1686 (−60)	89.9 (0.8)	1743 (−3)	127.3 (1.1)
hydroperoxyl HOO bend.	1383	37.7	1489 (106)	57.0 (1.5)	1478 (95)	51.4 (1.4)	1385 (2)	43.0 (1.1)
CH2 sym. bend.	1471	10.8	1464 (−7)	33.2 (3.1)	1460 (−11)	80.4 (7.4)	1470 (−1)	11.9 (1.1)
CH2O rock.	1215	11.0	1223 (8)	7.6 (0.7)	1211 (−4)	9.1 (0.8)	1212 (−3)	10.8 (1.0)
CH2(O) wagg.	1153	5.8	1174 (21)	6.4 (1.1)	1138 (−15)	1.3 (0.2)	1150 (−3)	4.8 (0.8)
hydroperoxyl OO stretch.	1124	28.5	1148 (24)	19.9 (0.7)	1173 (49)	30.0 (1.1)	1129 (5)	24.9 (0.9
intermolecular torsion			611	123.9	582	109.3	170	29.9
intermolecular bend.			228	47.5	320	7.4	102	115.9
intermolecular torsion			181	7.1	276	0.6	94	13.2
intermolecular torsion			160	0.6	232	44.8	45	13.7
intermolecular planar bend.			99	14.9	117	23.1	19	5.1
intermolecular torsion			65	11.1	86	16.3	4	0.3

[a] Scaled by a factor of 0.9614 to account for the anharmonic effects. [b] The frequency shifts relative to the separate reactants are given in parentheses. [c] The intensity ratios between the complex and the reactant are given in parentheses.

reactants side (see the ΔG values lying above the reactants). This is especially true for the **Cr1** and **Cr2** complexes because of their ring structures, which present ΔS values of 29.0 and 32.2 e.u., respectively, relative to the reactants (see Table 1), whereas, for the most weakly bonded van der Waals complex **Cr3**, a smaller differential entropic contribution is computed ($\Delta S = 12.2$ e.u., see Table 1). Consequently, the **Cr2** complex has an even higher ΔG value than that of the less-bonded **Cr3** complex (see Table 1). This important differential entropic effect is also clearly reflected in the corresponding equilibrium constants (K_{eq}), with computed values at 298 K of 4.37×10^{-21}, 4.62×10^{-23}, and 1.39×10^{-22} cm^3 $molecule^{-1}$ s^{-1} for **Cr1**, **Cr2**, and **Cr3**, respectively.

With the aim of helping the possible experimental identification of the pre-reactive complexes, we collected, in Table 2, the computed harmonic vibrational frequencies and IR intensities for the **Cr1**, **Cr2**, and **Cr3** complexes and for the H_2CO and HO_2 reactants as well. To account for the anharmonic effects, the computed frequencies were scaled by a factor of 0.9614, which was determined using the 6-31G(d) basis set at the same level of theory.[39] Table 2 also includes the frequency shifts corresponding to the difference between the vibrational frequency of the complex, the corresponding frequency of the isolated H_2CO or HO_2 reactants, and the ratios of the calculated intensity of the complex relative to the monomers. The computed frequencies of the **Cr1** complex were reported recently by Aloisio et al.,[16] and their values agree quite well with those of this work. For this complex, and in line with Aloisio's results, we calculated a red shift of 237 cm^{-1} for the HO stretching mode and a blue shift of 106 cm^{-1} for the HOO bend. Moreover, the intensities of these bands were found to be enhanced by factors of 24 and 1.5, respectively. Also interesting is the blue shift of 81 cm^{-1} computed for the CH_2 asymmetric stretching, which arises as a result of the O1$\cdots$H7C5 hydrogen bond interaction, although the IR intensity is computed to be reduced by a factor of 0.3. With regard to the complex **Cr2**, Table 2 shows that the computed red shift of the HO stretching is still larger (358 cm^{-1}), with an increase in the IR intensity of 4.2, while the HOO bend is blue-shifted by 95 cm^{-1}, and its intensity is enhanced by a factor of 1.4. Finally, the computed vibrational frequencies for the **Cr3** complex are practically the same as those of the separate reactants H_2CO and HO_2, according to the weak van der Waals-type interaction of this complex.

Radical Addition. We found four different transition structures, **TS1**, **TS4**, **TS5**, and **TS6**, (see Figures 3 and 4) for the radical addition channel. The reaction path having the lowest activation enthalpy occurs through **TS1** and has already been reported in the literature.[14,15,40,42] As shown in Figure 4, **TS1** has a five-membered-ring structure with C_S molecular symmetry, in which the corresponding electronic state is $^2A''$ ($13a'^2 3a''^2 4a''^1$), and the unpaired electron is located in an orbital perpendicular to the molecular plane. The main trends regarding the electronic features of this transition structure have been recently discussed in the literature,[40] and have allowed the process to be described as a proton-coupled electron-transfer (PCET) mechanism; that is, this elementary reaction involves the transfer of a "proton" (H3) of the hydroperoxyl moiety (O2) to the oxygen of the carbonyl group (O4), which occurs simultaneously with the addition of the terminal oxygen of HO_2 to the carbon of formaldehyde and an intermolecular electron transfer between the two oxygen atoms of the HO_2 moiety.[40] The result of this reaction is the formation of the peroxy radical $H_2C(OO)OH$ (**M3**, see Figure 3), according to eq 3. Figure 3 also shows that this reaction begins with the pre-reactive complex **Cr2** (C_S, $^2A''$). Here it is worth noting that this complex already has the symmetry, geometrical orientation, and electronic features of **TS1** (see above and Figures 1 and 4), so that the pre-reactive complex **Cr2** can be viewed as an "incipient proton-transfer reaction", as suggested by Steiner.[44] From an energetic point of view, the activation enthalpy, relative to **Cr2**, is computed to be 2.3 kcal/mol (see Table 1 and Figure 3), and our results predict **TS1** to be placed below the reactants ($\Delta E +$ ZPE $= -2.1$ kcal/mol or $\Delta H = -3.7$ kcal/mol; see Table 1). This energy value of -2.1 kcal/mol agrees very well with the -1.9 kcal/mol value reported recently by Dibble et al. at the CBS-QB3 level of theory[42] but less well with the -0.8 kcal/mol obtained at the RCCSD(T)/cc-pVTZ//CASSCf/6-311G(d,p) level of theory[15] or the -6.7 kcal/mol predicted at the BAC-MP4 level,[14] which points out the importance of the theoretical approach and basis set employed in obtaining accurate results. In addition, the reaction is computed to be exothermic by 16.8 kcal/mol (see Table 1), which agrees quite well with thermochemical estimates and theoretical results from the literature.[10,13−15,42]

There are two reaction paths, occurring through **TS5** and **TS4**, that lead to the formation of two conformers of the alkoxy radical $H_2C(O)OOH$ (**M2a** and **M2b**, respectively; see Figures

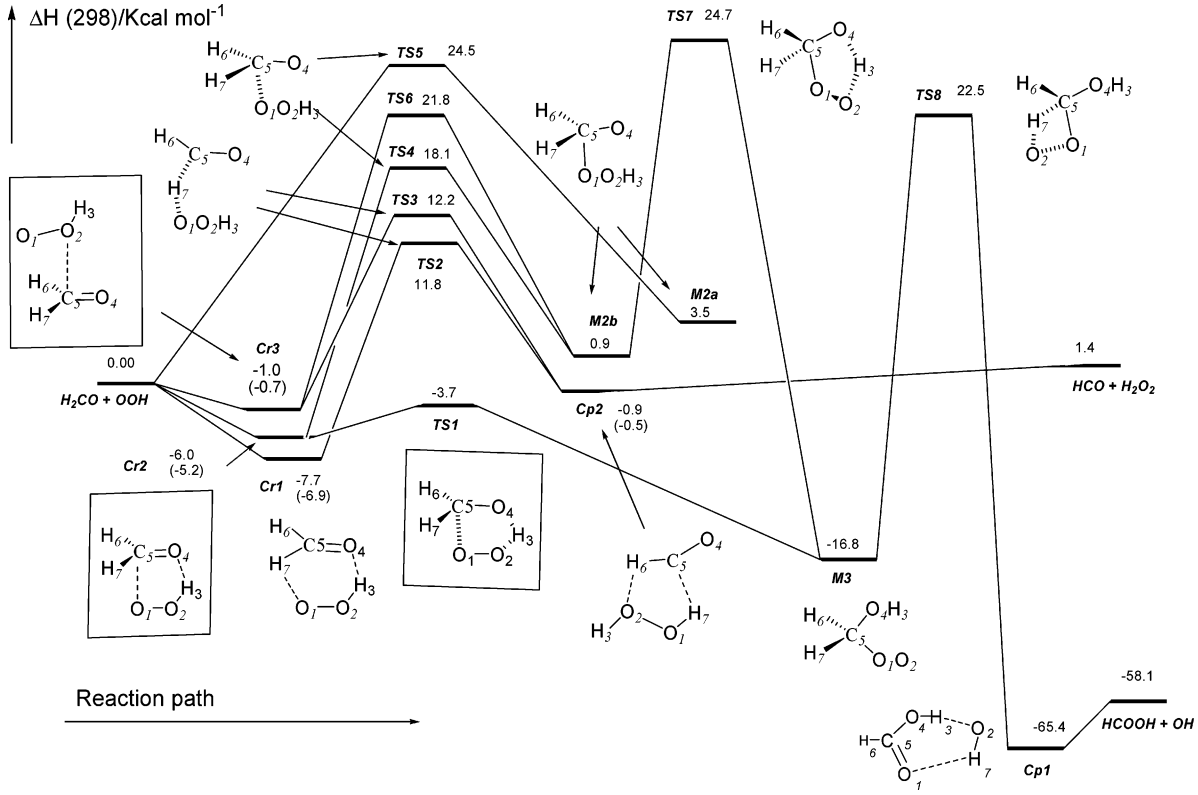

Figure 3. Schematic enthalpy diagram for the reaction between H_2CO and HO_2. Values in parentheses include BSSE corrections.

3 and 4), and, consequently, they correspond to the process indicated by eq 1. In the case of **TS4**, the reaction begins with the pre-reactive complex **Cr2**, whereas no pre-reactive complex was found for the elementary reaction through **TS5**. From an electronic point of view, both reaction paths involve a radical addition to the carbon atom of formaldehyde by interaction with the π bond of the carbonyl group, which is broken, and the unpaired electron in the corresponding $H_2C(O)OOH$ product is mainly located over the terminal oxygen from the carbonyl group. These facts are clearly reflected in the geometrical parameters of the corresponding conformers **M2a** and **M2b** (Figure 4), showing an increase in the length of the CO bond of 0.13−0.15 Å with respect to that of the carbonyl group in the formaldehyde reactant (Figure 1). Our results displayed in Table 1 and Figure 3 indicate that **M2b** is the most stable conformer of $H_2C(O)OOH$, and, moreover, it is energetically quasi-degenerate with the reactants ($\Delta H = 0.92$ kcal/mol), which is in good agreement with the thermochemical estimates from the literature.[10,13] For these elementary processes, our calculations predict very high activation enthalpies of 18.1 and 24.5 kcal/mol for **TS4** and **TS5**, respectively (see Table 1), which makes these processes unlikely. Here it is worth pointing out that these computed activation enthalpies are about 6−10 kcal/mol higher than those reported for the HO addition to formaldehyde.[7] Moreover, there is an additional unimolecular process going through **TS7**, which connects the alkoxy radical $H_2C(O)OOH$ (**M2b**) and the peroxy radical $H_2C(OO)OH$ (**M3**). This reaction is computed to be exothermic by 17.7 kcal/mol and requires a very high activation enthalpy ($\Delta H = 23.8$ kcal/mol, with respect to **M2b**; see Table 1 and Figure 3). In summary, the elementary steps $H_2CO + HO_2 \rightarrow$ **Cr2** $\rightarrow$ **TS4** $\rightarrow$ **M2b** $\rightarrow$ **TS7** $\rightarrow$ **M3** constitute a stepwise mechanism of eq 2. Geometric and energetic results for **TS4**, **M2b**, and **TS7** have been recently reported in the literature in connection with a study on the gas-phase oxidation of the hydroxymethyl radical by molecular oxygen,[15] and the reported values agree quite well with those in this work. Regarding the electronic features, and as pointed out very recently,[40] it is interesting to point out that the elementary reaction through **TS7** involves a hydrogen radical transfer from O2 to O4, and its higher activation barrier contrasts with the lower activation barrier computed for the PCET mechanism (via $H_2CO + HO_2 \rightarrow$ **Cr2** $\rightarrow$ **TS1** $\rightarrow$ **M3**; see Figure 3) described above for eq 2.

The reaction path going through **TS6** begins with the pre-reactive complex **Cr3**, and its result is the alkoxy radical $H_2C(O)OOH$ (**M2b**). The corresponding transition structure has C_S symmetry, and its electronic characterization is a $^2A''$ state ($13a'^2 3a''^2 4a''^1$) with the symmetry plane bisecting the H_2CO moiety, and we computed this transition state to lie 21.8 kcal/mol above the reactants. Behind the high activation energy for this step, it is interesting to pay attention to the geometrical and electronic features of **TS6** in comparison with those of **TS1**. Both transition structures have the same symmetry, the same electronic state ($^2A''$), and the same electronic description ($13a'^2 3a''^2 4a''^1$), with the unpaired electron located in an orbital perpendicular to the molecular plane, but differ from each other in the orientation of the hydrogen of the hydroperoxyl group (H3; see Figure 4). In **TS6**, the H3 is in a trans orientation with respect to the H_2CO moiety, which prevents this hydrogen from interacting with the oxygen (O4) of the carbonyl group. On the other side, the cis orientation of the H3 in **TS1** with respect to the H_2CO moiety (see Figure 4) allows this hydrogen to interact with O4 and consequently produce the PCET mechanism, which is energetically much more favored.

For the sake of completeness, we also looked for a reaction path involving the decomposition of **M3** into HCOOH + HO. Table 1 and Figure 3 show that the reaction is exothermic by 41.3 kcal/mol and that a hydrogen bond complex (**Cp1**; see Figure 3) is formed prior to the release of the products. The corresponding geometric and energy values for **Cp1**, formic acid, and hydroxyl radical were taken from the literature.[41] The transition structure of this reaction is labeled **TS8** in Figures 3

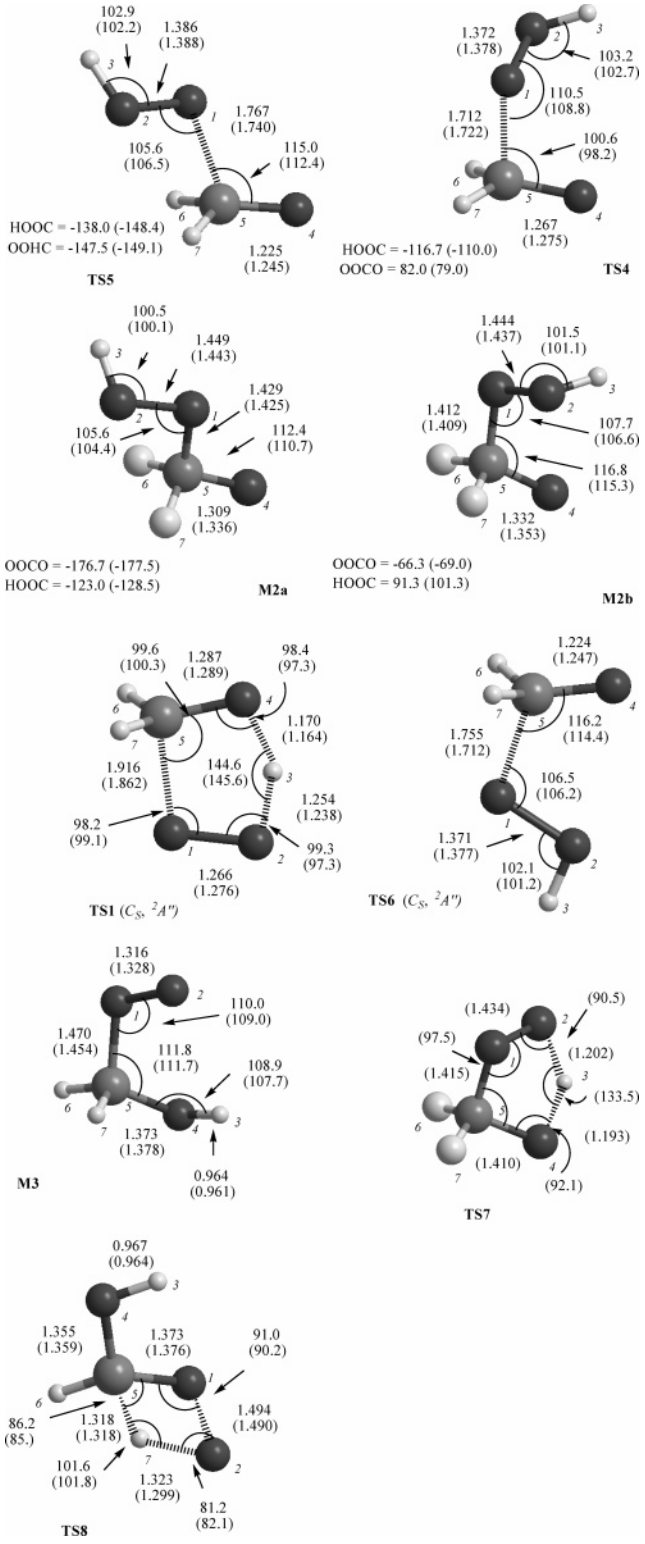

Figure 4. Selected geometrical parameters for the stationary points of the addition reaction, optimized at the B3LYP/6-311+G(2df,2p) and QCISD/6-311+G(d,p) (in parentheses) levels of theory.

and 4, and involves the simultaneous abstraction of H7 by the terminal oxygen (O2) of the peroxide group with the breakdown of the O1O2 bond in a highly strengthened four-membered-ring structure. The calculated activation enthalpy is very high (ΔH = 39.3 kcal/mol with respect to **M3**, see Figure 3), lessening the possible interest in this mechanism.

Hydrogen Abstraction. According to eq 3, the result of the hydrogen abstraction of formaldehyde by HO_2 is the formation

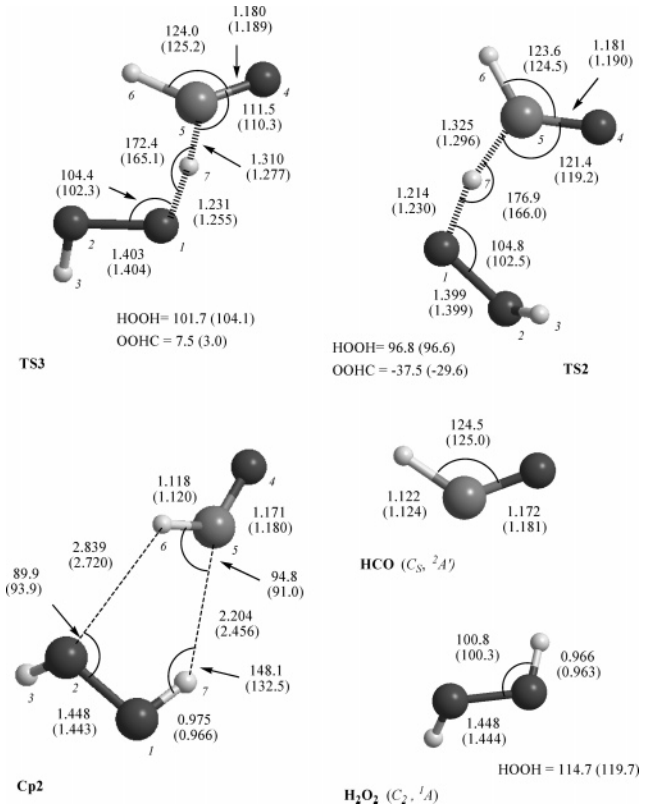

Figure 5. Selected geometrical parameters for the stationary points of the abstraction reaction, optimized at the B3LYP/6-311+G(2df,2p) and QCISD/6-311+G(d,p) (in parentheses) levels of theory.

of the HCO radical plus H_2O_2, and we computed this reaction to be slightly endothermic (ΔH = 1.4 kcal/mol; see Table 1).

We found two transition structures, **TS2** and **TS3**, (see Figure 5) for this process, which differ essentially in the relative orientation of the HOO moiety (cis or trans), with respect to the H_2CO moiety. Figure 5 shows that, in both stationary points, the hydrogen being transferred is slightly closer to the oxygen (about 1.23 Å) than to the C atom (about 1.32 Å), whereas the CO bond distances (about 1.19 Å) and the OO bond distances (about 1.40 Å) are closer to the corresponding bond lengths of the products ($HCO + H_2O_2$; see Figure 5) than to those of the reactants (H_2CO + HOO; see also Figure 1). Moreover, Figure 5 shows that the HOOH dihedral angle (between 97 and 104°) indicates that, in both transition states, the hydroperoxyl radical approaches formaldehyde in such a way that the electronic density of the unpaired electron is directed toward the hydrogen being abstracted. This geometric feature and a careful analysis of the wave function at the transition states show clearly that the process involves the transfer of the H radical so that the C5H7 and H7O1 bonds are broken and formed simultaneously.

From a mechanistic point of view, Figure 3 shows that, for each elementary process, the reaction begins with the formation of a hydrogen-bonded complex prior to the transition state (**Cr1** and **Cr3** for **TS2** and **TS3**, respectively), and a common product complex (**Cp2**) is formed before the release of the HCO and HOOH products. The most relevant geometric features of the **Cp2** complex are also displayed in Figure 5.

Regarding the energy of the reaction, Table 1 and Figure 3 show that the computed activation enthalpies for **TS2** and **TS3** are 11.8 and 12.2 kcal/mol, respectively, with respect to the reactants, but, if considering the pre-reactive complexes, the activation enthalpies in the corresponding unimolecular processes are 19.5 and 13.2 kcal/mol for **TS2** and **TS3**, respectively.

TABLE 3: Calculated Values, at Different Temperatures, of the Equilibrium Constant of Cr2 (K_{eq}), Tunneling Parameter (κ), Unimolecular Rate Constant (k_2), and Total Rate Constant (K_{TS1}) for TS1

T	250	280	298	300	320	340	360	380	400
K_{eq}[a]	2.10×10^{-22}	7.62×10^{-23}	4.62×10^{-23}	4.38×10^{-23}	2.73×10^{-23}	1.81×10^{-23}	1.26×10^{-23}	9.21×10^{-24}	6.99×10^{-24}
κ	1.6734	1.406	1.2949	1.2841	1.1901	1.1155	1.0551	1.0051	1.0[b]
k_2[c]	1.02×10^{9}	1.63×10^{9}	2.07×10^{9}	2.12×10^{9}	2.65×10^{9}	3.23×10^{9}	3.85×10^{9}	4.50×10^{9}	5.18×10^{9}
K_{TS1}[a]	2.15×10^{-13}	1.25×10^{-13}	9.54×10^{-14}	9.28×10^{-14}	7.23×10^{-14}	5.84×10^{-14}	4.86×10^{-14}	4.15×10^{-14}	3.61×10^{-14}

[a] In cm^3 $molecule^{-1}$ s^{-1}. [b] The tunneling is < 1 and is therefore not considered. [c] In s^{-1}.

TABLE 4: Calculated Values, at Different Temperatures, of the Equilibrium Constant (K_{Eq}), Tunneling Parameter (κ), Unimolecular Rate Constant (k_2), and Total Rate Constant (K_{TS}) for the Hydrogen Abstraction Reaction

T	298	500	600	700	800	900	1000
K_{eq-Cr1}[a]	4.37×10^{-21}	7.74×10^{-23}	3.30×10^{-23}	1.91×10^{-23}	1.34×10^{-23}	1.05×10^{-23}	8.96×10^{-24}
κ	19.771	2.0174	1.4557	1.1898	1.0372	1[b]	1[b]
k_2[c]	1.74×10^{-1}	1.67×10^{4}	3.74×10^{5}	3.65×10^{6}	2.09×10^{7}	8.79×10^{7}	2.89×10^{8}
K_{TS2}[a]	7.58×10^{-22}	1.29×10^{-18}	1.23×10^{-17}	6.99×10^{-17}	2.79×10^{-16}	9.24×10^{-16}	2.59×10^{-15}
K_{eq-Cr3}[a]	1.39×10^{-22}	1.81×10^{-22}	2.27×10^{-22}	2.86×10^{-22}	3.60×10^{-22}	4.48×10^{-22}	5.53×10^{-22}
κ	15.972	1.9324	1.414	1.1642	1.0194	1[b]	1[b]
k_2[c]	4.97	7.77×10^{3}	6.02×10^{4}	2.73×10^{5}	8.70×10^{5}	2.36×10^{6}	5.36×10^{6}
K_{TS3}[a]	6.89×10^{-22}	1.40×10^{-18}	1.37×10^{-17}	7.81×10^{-17}	3.13×10^{-16}	1.06×10^{-15}	2.96×10^{-15}
				$K_{TOTAL} = K_{TS2} + K_{TS3}$			
K_{TOTAL}	1.45×10^{-21}	2.69×10^{-18}	2.60×10^{-17}	1.48×10^{-16}	5.92×10^{-16}	1.98×10^{-15}	5.55×10^{-15}

[a] In cm^3 $molecule^{-1}$ s^{-1}. [b] The tunneling is < 1 and is therefore not considered. [c] In s^{-1}.

The product complex **Cp2** is computed to be quasi-degenerate with the reactants ($\Delta H = -0.9$ kcal/mol, or -0.5 kcal/mol when the BSSE correction is considered; see Table 1). At this point, it is worth comparing the gas-phase oxidation of formaldehyde by hydroperoxyl radical discussed in this work with the corresponding oxidation by hydroxyl radical that was reported recently by Alvarez-Idaboy et al.[7] The reaction of H_2CO with HO_2 radical occurs through a complex PCET mechanism (via **TS1**), which involves the addition of the terminal oxygen of the HO_2 to the carbon of the formaldehyde and a simultaneous transfer of the proton of the radical to the oxygen of the carbonyl, whereas the hydrogen abstraction of formaldehyde requires a much higher activation energy (via **TS2** and **TS3**). On the other side, the reaction of H_2CO with HO radical occurs by the abstraction of an hydrogen atom of the aldehyde in a process with a computed activation barrier of 3.19 kcal/mol.[7]

Kinetics. For the shake of completeness, we carried out rate constant calculations at different temperatures on the processes described by eqs 2 and 3 by using conventional transition-state theory. The main goal at this point is to analyze whether the results obtained in this work are able to predict the negative temperature dependence observed experimentally. Figure 3 shows clearly that the processes pointed out by eqs 2 and 3 correspond to a complex reaction involving the formation of a pre-reactive complex prior to the transition state, as described by eq 4, and the rate constants were calculated according eq 5. Here it is important to know which K_{eq} should be considered, especially for **TS1**, because the lowest lying complex is **Cr1**. Although **TS1** connects with **Cr2**, the geometric and electronic features of both complexes (see above) suggest that a transition state should exist connecting them, and therefore one would expect to consider the K_{eq} of **Cr1**. However, we were unable to find such a transition state, and therefore we decided to consider the K_{eq} of **Cr2** for **TS1**, the K_{eq} of **Cr1** for **TS2**, and the K_{eq} of **Cr3** for **TS3**. In each case, we took the best computed energy values, (CCSD(T)/aug-cc-pVTZ), whereas the partition functions employed were those computed at B3LYP/6-311+G(2df,2p). For the equilibrium constant calculations, the BSSE correction for the relative stability between the reactants and the complexes were taken into account.

Table 3 shows the computed rate constants for the reaction occurring through eq 2 at temperatures between 250 and 400 K, in which a small tunneling contribution is observed. The rate constant computed at 300 K is 9.28×10^{-14} cm^3 $molecule^{-1}$ s^{-1}, which agrees quite well with the range of $4.96-7.8 \times 10^{-14}$ cm^3 $molecule^{-1}$ s^{-1} reported experimentally.[1,6,8-11] More importantly, the negative temperature dependence of the rate constant is also reasonably well described, as we derived a rate expression of 1.85×10^{-15} (cm^3 $molecule^{-1}$ s^{-1}) exp(2.35(kcal/mol)/RT), compared with the experimentally derived 6.71×10^{-15} (cm^3 $molecule^{-1}$ s^{-1}) exp(1.19($\pm$1.19 kcal/mol)/RT); 7.69×10^{-15} (cm^3 $molecule^{-1}$ s^{-1}) exp(1.24($\pm$1.09 kcal/mol)/RT) and 9.71×10^{-15} (cm^3 $molecule^{-1}$ s^{-1}) exp(1.24($\pm$1.19kcal/mol)/RT.[1,6,8-11]

With regard to the formation of $HCO + H_2O_2$ (eq 3), which is of interest in combustion chemistry, we calculated the rate constant in the 298−1000 K temperature range, and the corresponding values were collected in Table 4. In this case, there are two types of processes describing eq 3, namely, those occurring through **Cr1** and **TS2** and those occurring through **Cr3** and **TS3**, with nearly equal contribution to the rate constant (see Table 4). The overall K value computed at 700 K is 1.48×10^{-16} cm^3 $molecule^{-1}$ s^{-1}, in comparison with the range of $4.13-7.54 \times 10^{-16}$ cm^3 $molecule^{-1}$ s^{-1} reported experimentally.[6,17-19]

Conclusions

The theoretical study carried out in this work lead to the following conclusions:

1. There are three pre-reactive complexes (**Cr1**, **Cr2**, and **Cr3**), formed between formaldehyde and hydroperoxyl radical. The most stable complex, **Cr1**, lying 6.9 kcal/mol below the sum of the enthalpies of the reactants, is stabilized by two hydrogen bonds. The **Cr2** complex, lying 5.2 kcal/mol below the reactants, is bonded by one hydrogen bond and one van der Waals interaction, whereas **Cr3** is computed to be more stable than the reactants by only 0.7 kcal/mol and has a van der Waals interaction only.

2. The present work confirms that the result of the reaction between H_2CO and HO_2 is the peroxy radical $CH_2(OO)OH$, according to eq 2, for which we calculated a reaction enthalpy of 16.8 kcal/mol at 298 K. However, the reaction mechanism is complex and occurs through the formation of a pre-reactive

complex, which is formed prior to the transition state **TS1**. The pre-reactive complex and the transition state lie energetically below the sum of the enthalpies of the reactants by 5.2 and 3.7 kcal/mol, respectively. Moreover, the analysis of the wave function at the transition structure shows that the process occurs through a PCET mechanism.

3. The kinetic study carried out in this work predicts a rate constant of 9.28×10^{-14} cm^3 molecule^{-1} s^{-1} at 300 K for reaction 2, which is in reasonable agreement with the experimental values. Moreover, the calculations also predict reasonably well the negative temperature dependence of the rate constant.

4. We found three reaction paths for the HO_2 radical addition to the π bond of the carbonyl (**TS4**, **TS5**, and **TS6**), and our calculations show that the computed activation enthalpies are higher than 18 kcal/mol, making these processes unlikely.

5. For the hydrogen abstraction of eq 3, which is of interest in combustion processes, we found two different reaction paths, in which the corresponding transition structures differ from each other in a conformational change. In both paths, the reaction begins with the formation of a pre-reactive complex, and we computed activation enthalpies of 11.8 and 12.2 kcal/mol (for **TS3** and **TS2**, respectively), with respect to the reactants. Our computed rate constant at 700 K was 1.48×10^{-16} cm^3 molecule^{-1} s^{-1}, which agrees reasonably well with experimental results.

6. There is a great difference in the reactivity of H_2CO with HO_2 and that with HO radicals. Whereas hydroxyl radical reacts with formaldehyde by extracting an aldehydic hydrogen,[7] the reaction of H_2CO with hydroperoxyl radical proceeds through a more complex mechanism involving a PCET process.

Acknowledgment. The financial support for this research was provided by the Dirección General de Investigación Científica y Técnica (DGYCIT, Grant BQU2002-0485-C02-01) and by the Generalitat de Catalunya (Grant 2001SGR00048). The calculations described in this work were carried out at the Centre de Supercomputació de Catalunya (CESCA) and the Centro de Supercomputación de Galicia (CESGA), whose services are gratefully acknowledged. We are indebted to Profs. Olivella, Bofill, and Solé for helpful discussions.

Supporting Information Available: Absolute energy values, topological parameters of selected stationary points, rotational constants for the pre-reactive complexes, and the optimized geometries. This material is available free of charge via the Internet at http://pubs.acs.org.

References and Notes

(1) Carlier, P.; Hannachi, H.; Mouvier, G. *Atmos. Environ.* **1986**, *20*, 2079.
(2) Altshuller, A. *Atmos. Environ., Part A* **1993**, *27*, 2131.
(3) Carter, W. P. L. *J. Air Waste Manage. Assoc.* **1994**, *44*, 881.
(4) Grosjean, D. *Environ. Sci. Technol.* **1991**, *25*, 710.
(5) Grosjean, D.; Miguel, D. A. H.; Tavares, T. M. *Atmos. Environ., Part B* **1990**, *24*, 101.
(6) NIST Chemical Kinetics Database on the Web, Standard Reference Database 17, Version 7.0 (Web Version), Release 1.3. http://kinetics.nist.gov/index.php (accessed April 2005).
(7) Alvarez-Idaboy, J. R.; Mora-Diez, N.; Boyd, R. J.; Vivier-Bunge, A. *J. Am. Chem. Soc.* **2001**, *123*, 2018.
(8) Veyret, B.; Rayez, J.-C.; Lesclaux, R. *J. Phys. Chem.* **1982**, *86*, 3424.
(9) Veyret, B.; Lesclaux, R.; Rayez, M.-T.; Rayez, J.-C.; Cox, R. A.; Moortgat, G. K. *J. Phys. Chem.* **1989**, *93*, 2368.
(10) Zabel, F.; Sahetchian, K. A.; Chachaty, C. *Chem. Phys. Lett.* **1987**, *134*, 433.
(11) Atkinson, R.; Baulch, D. L.; Cox, R. A.; Hampson, R. F.; Jr., J. A. K.; Rossi, M. J.; Troe, J. *J. Phys. Chem. Ref. Data* **1997**, *26*, 521.
(12) Su, F.; Calvert, J. G.; Shaw, J. H. *J. Phys. Chem.* **1979**, *83*, 3185.
(13) Benson, S. W. *Int. J. Chem. Kinet.* **2001**, *33*, 509.
(14) Evleth, E. M.; Melius, J. C. F.; Rayez, M. T.; Rayez, J. C.; Forsts, W. *J. Phys. Chem.* **1993**, *97*, 5040.
(15) Olivella, S.; Bofill, J. M.; Solé, A. *Chem.—Eur. J.* **2001**, *7*, 3377.
(16) Aloisio, S.; Francisco, J. S. *J. Phys. Chem. A* **2000**, *104*, 3211.
(17) Eiteneer, B.; Yu, C.-L.; Goldenberg, M.; Frenklach, M. *J. Phys. Chem. A* **1998**, *102*, 5196.
(18) Jemi-Alade, A.; Lightfoot, P. D.; Lesclaux, R. *Chem. Phys. Lett.* **1992**, *195*, 25.
(19) Baulch, D. L.; Cobos, C. J.; Cox, R. A.; Esser, C.; Frank, P.; Just, T.; Kerr, J. A.; Pilling, M. J.; Troe, J.; Walker, R. W.; Warnatz, J. *J. Phys. Chem. Ref. Data* **1992**, *21*, 411.
(20) Becke, A. D. *J. Chem. Phys.* **1993**, *98*, 5648.
(21) Frisch, M. J.; Pople, J. A.; Binkley, J. S. *J. Chem. Phys.* **1984**, *80*, 3265.
(22) Hehre, W. J.; Radom, L.; Schleyer, P. v. R.; Pople, J. A. In *Ab Initio Molecular Orbital Theory*; John Wiley: New York, 1986; p 86.
(23) Ishida, K.; Morokuma, K.; Kormornicki, A. *J. Chem. Phys.* **1977**, *66*, 2153.
(24) Gonzalez, C.; Schlegel, H. B. *J. Chem. Phys.* **1989**, *90*, 2154.
(25) Gonzalez, C.; Schlegel, H. B. *J. Phys. Chem.* **1990**, *94*, 5523.
(26) Pople, J. A.; Head-Gordon, M.; Raghavachari, K. *J. Chem. Phys.* **1987**, *87*, 5968.
(27) Cizek, J. *Adv. Chem. Phys.* **1969**, *14*, 35.
(28) Barlett, R. J. *J. Phys. Chem.* **1989**, *93*, 1963.
(29) Dunning, T. H. J. *J. Chem. Phys.* **1989**, *90*, 1007.
(30) Kendall, R. A.; Dunning, T. H., Jr.; Harrison, R. J. *Chem. Phys* **1992**, 6769.
(31) Lee, T. J.; Taylor, P. R. *Int. J. Quantum Chem. Symp.* **1989**, *23*, 199.
(32) Rienstra-Kiracofe, J. C.; Allen, W. D.; Schaefer, H. F., III *J. Phys. Chem. A* **2000**, *104*, 9823.
(33) Boys, S. F.; Bernardi, F. *Mol. Phys.* **1970**, *19*, 553.
(34) Frisch, M. J.; Trucks, G. W.; Schlegel, H. B.; Scuseria, G. E.; Robb, M. A.; Cheeseman, J. R.; Zakrzewsk, V. G.; Montgomery, J. A., Jr.; Stratmann, R. E.; Buran, J. C.; Dapprich, S.; Millam, J. M.; Daniels, A. D.; Kudin, K. N.; Strain, M. C.; Farkas, O.; Tomasi, J.; Barone, V.; Cossi, M.; Cammi, R.; Mennucci, B.; Pomelli, C.; Adamo, C.; Clifford, S.; Ochterski, J.; Petersson, G. A.; Ayala, P. Y.; Cui, Q.; Morokuma, K.; Rega, N.; Salvador, P.; Dannenberg, J. J.; Malick, D. K.; Rabuck, A. D.; Raghavachari, K.; Foresman, J. B.; Cioslowski, J.; Ortiz, V.; Baboul, A. G.; Stefanov, B. B.; Liu, G.; Liashenko, A.; Piskorz, P.; Komaromi, I.; Martin, R. G. L.; Fox, D. J.; Keith, T.; Al-Laham, M. A.; Peng, C. Y.; Nanayakkara, A.; Challacombe, M.; Gill, P. M. W.; Johnson, B.; Chen, W.; Wong, M. W.; Andres, J. L.; Gonzalez, C.; Head-Gordon, M.; Replogle, E. S.; Pople, J. A. *Gaussian 02*; Gaussian, Inc.: Pittsburgh, PA, 2002.
(35) Shaftenaar, G.; Noordik, J. H. *J. Comput.-Aided Mol. Des.* **2000**, *14*, 123.
(36) Bader, R. F. W. *Atoms in Molecules. A Quantum theory*; Clarendon Press: Oxford, 1995; Vol. 22.
(37) Bader, R. F. W. http://www.chemistry.mcmaster.ca/aimpac (accessed May 2002).
(38) Duncan, W. T.; Troung, T. N. http://therate.hec.utah.edu (accessed September 2000).
(39) Scott, A. P.; Radom, L. *J. Phys. Chem.* **1996**, *100*, 16502.
(40) Olivella, S.; Anglada, J. M.; Sole, A.; Bofill, J. M. *Chem.—Eur. J.* **2004**, *10*, 3404.
(41) Anglada, J. M. *J. Am. Chem. Soc.* **2004**, *126*, 9809.
(42) Dibble, T. S. *Chem. Phys. Lett.* **2002**, *355*, 193.
(43) Truong, T. N.; Truhlar, D. G. *J. Chem. Phys.* **1990**, *93*, 1761.
(44) Steiner, T. *Angew. Chem., Int. Ed.* **2002**, *41*, 48.
(45) At the MP2/6-311+G(2df, 2p) level of theory, the H3O4 and O1C5 bond distances of **Cr2** are computed to be 1.805 and 2.621 Å, respectively. The Cartesian coordinates are given as Supporting Information.